AIP | Applied Physics Letters

Integrated high-quality factor silicon-on-sapphire ring resonators for the mid-infrared

Raji Shankar, Irfan Bulu, and Marko Lončar

Citation: Appl. Phys. Lett. **102**, 051108 (2013); doi: 10.1063/1.4791558
View online: http://dx.doi.org/10.1063/1.4791558
View Table of Contents: http://apl.aip.org/resource/1/APPLAB/v102/i5
Published by the American Institute of Physics.

Integrated high-quality factor silicon-on-sapphire ring resonators for the mid-infrared

Raji Shankar,[a] Irfan Bulu, and Marko Lončar
School of Engineering and Applied Sciences, Harvard University, Cambridge, Massachusetts 02138, USA

(Received 9 December 2012; accepted 28 January 2013; published online 7 February 2013)

We demonstrate high-quality (Q) factor grating-coupled ring resonators in a silicon-on-sapphire platform, operating at wavelengths between 4.3 and 4.6 μm. Total Q-factors of 151 000 and intrinsic Q-factors of 278 000 are measured, representing the highest Q-factors measured at the mid-infrared in Si. © *2013 American Institute of Physics*. [http://dx.doi.org/10.1063/1.4791558]

The mid-infrared (IR) wavelength region (2–20 μm) is of great interest for a variety of applications as wide-ranging as trace gas sensing, free-space communications, and thermal imaging. While high-power sources and sensitive detectors at the mid-IR range have finally reached maturity, the passive photonic devices needed to properly access these applications on-chip are still a work in progress.

Silicon has previously been proposed as an ideal material for the mid-IR[1,2] due to its low material losses below 8 μm. Additionally, due to the absence of two- or even three-photon absorption, the mid-IR wavelengths offer us the opportunity to efficiently exploit the optical nonlinearities of Si, opening up a whole host of applications in nonlinear wavelength conversion and signal amplification. However, the traditional silicon-on-insulator (SOI) platform is of limited utility at these wavelengths, since SiO_2 is a highly lossy material in the mid-IR, with losses of over 2 dB/cm at wavelengths longer than 3.5 μm.[1,3] While our group has previously demonstrated Si membrane photonic crystal cavities (PhCs) operating at 4.5 μm,[4,5] many mid-IR photonics applications will require an integrated, on-substrate platform. Also, applications in nonlinear optics require higher in-coupled powers than those attainable through the free-space coupling method employed in Refs. 4 and 5. Silicon-on-sapphire (SOS) provides an attractive platform for on-substrate mid-infrared photonics, due to the low loss of sapphire through much of the mid-IR.[1,2] SOS waveguides operating at 2.75 μm,[6] 4.5 μm,[7] 5.18 μm,[8] and 5.5 μm,[9] microring resonators operating at 2.75 μm[10] and 5.5 μm,[9] and grating couplers operating at 2.75 μm[6,10] have already been demonstrated. In this paper, we demonstrate grating-coupled SOS microring resonators operating in the 4.3–4.6 μm range, with loaded quality (Q) factors of 151 000 and intrinsic Q-factors of 278 000.

Coupling high optical powers into MIR resonators has proven to be a challenging task,[4,7,9] The fiber-coupling inverse taper method of spot size conversion[11] commonly used at telecommunications (telecom) wavelengths is difficult to achieve with high efficiency, due to the immaturity of fiber technology at the mid-infrared. Grating couplers, on the other hand, can provide highly efficient coupling of light from a free space beam into an optical waveguide. This method has already been well studied at the telecom wavelengths, with experimentally measured coupling losses as low as −1.6 dB.[12,13] Additionally, grating couplers can be placed anywhere on the chip, affording flexibility in input/output coupling location. For these reasons, we chose to use grating couplers to couple light into our ring resonators. The grating coupler was optimized in Comsol using NOMAD,[14] a global optimization algorithm. A linear taper function was applied both to the periodicity and the duty cycle of the grating structure. The theoretical coupling efficiency of the optimized grating at normal incidence for a fully etched geometry was 40%, with a bandwidth of about 150 nm. We note that coupling efficiencies in excess of 70% are possible at larger incidence angles. On the output end, light was collected from the cleaved end facet of the output waveguide. This simplifies the experimental setup considerably and allows for fast device characterization.

The devices were fabricated on a silicon-on-sapphire substrate with a device layer thickness of 812 nm (IQEP Silicon, Ltd.). ZEP (Zeon Corp.) was used as a mask for electron-beam lithography. A standard 125 kV electron-beam lithography tool (Elionix F-125) was used to define patterns in the ZEP layer, which were then developed in o-xylene for 40 s followed by an isopropanol alcohol rinse. A single step etch process was performed in a reactive ion etcher (STS ICP RIE) using C_4F_8 and SF_6 gases. Finally, the sample was manually cleaved on the output waveguide, providing an end facet for out-coupling.

An optical micrograph of one of our devices is shown in Figure 1. The grating coupler, taper region, ridge waveguide, and ring resonator all are fully etched into the Si device layer with thickness $t = 812$ nm. The coupling waveguide and ring resonator both have a width $w = 1.5$ μm, and the ring radius $r = 60$ μm. The grating slits are 50 μm wide, and the taper region between the grating and coupling waveguide is 500 μm long. Rings with gaps d between the coupling waveguide and ring resonator varying between 300 and 700 nm were fabricated. Since the bandwidth of the grating is smaller than the mode-hop free tuning range of our laser, the grating geometry was varied from device to device in order to cover the laser's tuning range. This was done by multiplying each grating dimension with a constant in the range of 0.98 to 1.06, which shifts the center wavelength of the grating by the same factor.

A horn-shaped coupler consisting of a 750 μm long linear taper with a width of 50 μm at the output end was used to

[a]Author to whom correspondence should be addressed. Electronic mail: shankar2@fas.harvard.edu.

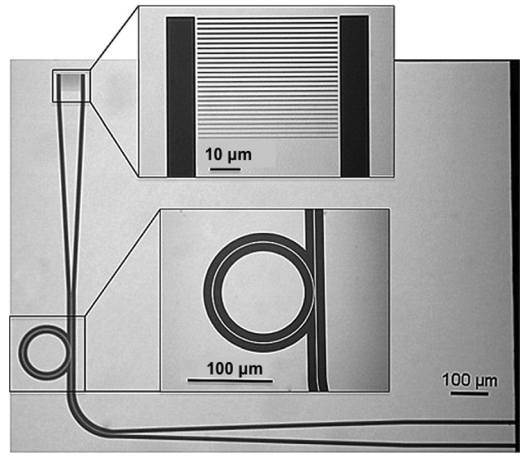

FIG. 1. Optical image of a representative device, consisting of a ring resonator (bottom inset) coupled to a waveguide with a grating coupler (top inset) on input end and horn-coupler on the output end.

improve collection of light at the output. By using this approach,[7,9] we were able to increase out-coupling efficiency from 9% (for a 1.6 μm waveguide without a horn) to 25%, assuming a lens with numerical aperture of 0.5.

The setup used to characterize our devices is shown in Figure 2. Light from a tunable continous-wave quantum cascade laser (QCL) from Daylight Solutions, Inc., with emission from 4.27 to 4.63 μm and linewidth of <45 MHz, is sent through a ZnSe objective (numerical aperture of 0.22) and focused onto the input grating. A second ZnSe lens (numerical aperture of 0.5) is placed at right angle to the first lens in order to collect light from the end facet. Finally, the light is focused onto a thermoelectrically cooled HgCdTe (MCT) detector.

Transmission data from our as-processed ring resonators are shown in Figure 3(a). Results from a device with a value of $d = 300$ nm is shown. Resonances were also measured in devices with $d = 400$ nm and 550 nm, with no resonances seen for $d = 700$ nm. The free spectral range (FSR) of our resonators was measured to be 12.4 nm around 4.4 μm, which closely matches the expected FSR of a ring with radius $r = 60$ μm and theoretical group waveguide index of 4.1 at 4.4 μm. For a ring resonator coupled to a waveguide, the total (loaded) Q-factor Q_t is given by the relation $Q_t^{-1} = Q_0^{-1} + Q_c^{-1}$, where Q_0 is the intrinsic Q-factor (determined by radiation losses

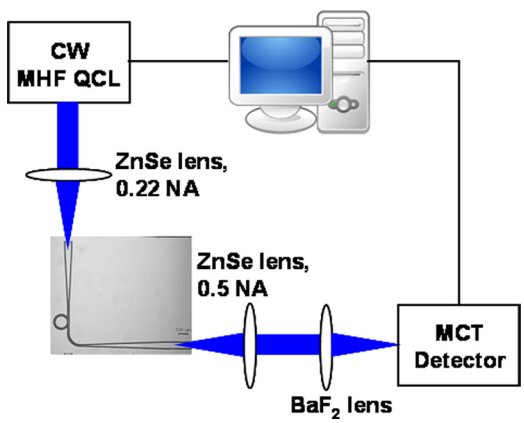

FIG. 2. Schematic of experimental setup used to characterize our devices in transmission.

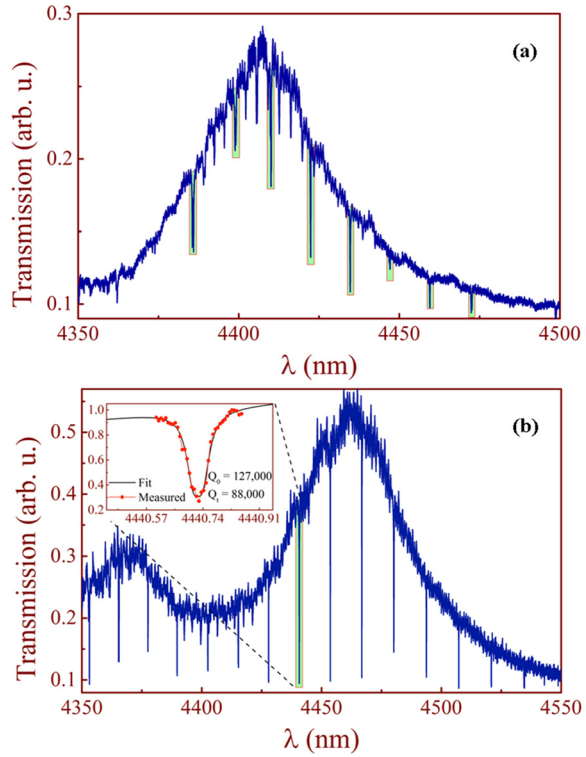

FIG. 3. (a) Transmission measurement of device with coupling gap $d = 300$ nm, as fabricated. Ring resonances are highlighted with green to distinguish them from gas absorption dips (from atmospheric $C_{13}O_2$). (b) Device with $d = 300$ nm, after Piranha etch/HF cycling (Note: (a) and (b) are on same sample, but are not the same device.) Power transfer between the waveguide and the ring is greatly improved, and maximum loaded Q-factors have increased from 45 000 to 94 000, with a maximum intrinsic Q-factor of 127 000, shown in the inset.

and material absorption, including surface states) of the ring resonator, and Q_c is the coupling Q-factor (determined by the coupling strength with the waveguide). Power transfer between the waveguide and the ring resonator is maximized when $Q_0 = Q_c$, a regime known as critical coupling. For $Q_0 < Q_c$, the ring resonator is considered undercoupled, and for $Q_0 > Q_c$, the ring resonator is considered overcoupled. In our measurements, the coupling decreased with increasing d, indicating that our devices operate in the undercoupling regime. The experimentally obtained transmission spectra were fitted to theoretical curves obtained by solving a set of coupled mode equations[15] that take into account the scattering-induced coupling of clock-wise and counter-clock-wise propagating modes, which can be observed as mode-splitting for very high-Q resonators. Using this approach, we inferred maximum loaded Q values of $Q_t = 41\,000$ and intrinsic Q-factors of $Q_0 = 45\,000$. In order to improve the performance of our devices, we decided to subject them to the post-fabrication microelectronic treatments described in Refs. 5 and 16, namely Piranha etch/HF cycling and annealing. The former treatment decreases absorption due to surface states and reduces surface roughness, while the latter treatment reduces absorption due to water.[5] A cycle of Piranha etch (3:1 H_2SO_4:H_2O_2) and HF acid performed three times in succession (process detailed in Ref. 16) had the most dramatic effect (annealing had limited effect on these devices), increasing loaded Qs to as much as 94 000 and drastically improving the coupling across all

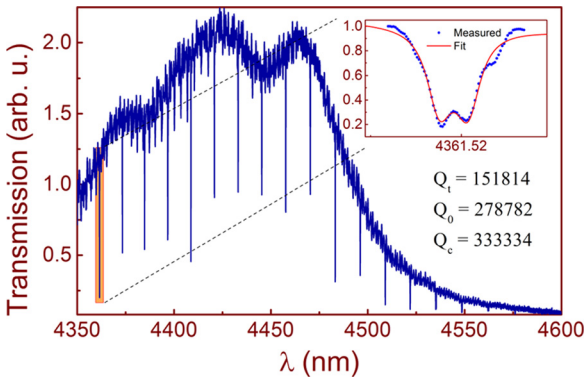

FIG. 4. Transmission measurement of device with $d = 300$ nm, fabricated using resist reflow and post-fabrication Piranha-HF cycling. The reflow results in higher Q-factors, with a maximum loaded Q_t of 151 000 and intrinsic Q_0 of 278 000, as shown in the inset.

devices. The response from one of the best devices (with $d = 300$ nm) is seen in Figure 3(b). After post-processing, we were also able to see resonances for devices with $d = 700$ nm, indicating that Q_0 for these devices had increased with respect to Q_c. From fitting the transmission spectrum, we deduced intrinsic Q-factors as high as $Q_0 = 127\,000$ (see inset, Figure 3(b)).

To minimize scattering losses due to fabrication imperfections, we applied the resist reflow method to our devices.[17] In our case, resist reflow consisted of a 5-min post-lithography bake in an oven at 140 °C. Because of the fine features within our grating couplers, we had to use lower bake temperatures for reflow than those typically used for microresonators.[17] After the reflow, the sample underwent etching, cleaving, and Piranha etch-HF acid cycling as described above. The results are shown in Figure 4. Q-factors increased noticeably after the reflow, with total Q-factors as high as $Q_t = 151\,000$, corresponding to a resonance linewidth of 440 MHz, and intrinsic Q-factors as high as $Q_0 = 278\,000$. These Q-values are the highest measured in the 4–5 μm wavelength range in Si. We note that for all device geometries we tested (a total of 12), Q-factors obtained with resist reflow were higher than Qs of the devices where the reflow was not used.

Using our Q values, we can estimate the loss of our ring resonators to be about 0.74 dB/cm at 4.5 μm. We note that this loss value takes into account light scattering (due to surface roughness) and material absorption (due mostly to surface states), and also bending losses of the ring resonator (which are negligible in large diameter devices that we studied). This is slightly higher than the lowest waveguide loss values measured in silicon devices at the mid-IR (0.6 dB/cm at 3.39 μm in the case of SOI waveguides).[18] Our comparatively higher losses may be due to scattering losses from twinning defects inherent in SOS.[19]

In conclusion, we have realized mid-IR integrated on-chip optical networks operating at the 4.5 μm wavelength range, based on the SOS material platform. Grating-coupled ring resonators, with intrinsic Q-factors as high as 278 000, were demonstrated. High Q-factor resonators in the mid-IR are of great interest for trace-gas sensing in particular, and the realization of portable spectroscopy systems in general. Another exciting application of our platform is on-chip nonlinear wavelength conversion via four-wave mixing, as well as the potential realization of chip-scale frequency combs operating in the mid-IR.

This work was partially funded by SBIR Contract W911SR-11-C-0008 from the U. S. Army. The authors would like to thank Mickey Frish (Physical Sciences Incorporated) for fruitful discussions and Julie Frish for her assistance in acid preparation. Device fabrication was performed at the Center for Nanoscale Science at Harvard University.

[1]R. Soref, Nat. Photonics **4**(8), 495 (2010).
[2]R. A. Soref, S. J. Emelett, and A. R. Buchwald, J. Opt. A **8**(10), 840 (2006).
[3]M. Nedeljkovic, M. Milosevic, T. Ben Masaud, E. Jaberansary, H. Chong, N. Emerson, G. Reed, and G. Mashanovich, Appl. Phys. Lett. **101**(12), 121105 (2012).
[4]R. Shankar, R. Leijssen, I. Bulu, and M. Loncar, Opt. Express **19**(6), 5579 (2011).
[5]R. Shankar, I. Bulu, R. Leijssen, and M. Loncar, Opt. Express **19**(24), 24828 (2011).
[6]X. Chen Z. Cheng, C. Y. Wong, K. Xu, C. Fung, Y. Chen, and H. K. Tsang, IEEE Photon. J. **4**(1), 104 (2012).
[7]T. Baehr-Jones, A. Spott, R. Ilic, A. Spott, B. Penkov, W. Asher, and M. Hochberg, Opt. Express **18**(12), 12127 (2010).
[8]F. Li, S. D. Jackson, C. Grillet, E. Magi, D. Hudson, S. J. Madden, Y. Moghe, C. O'Brien, A. Read, S. G. Duvall, P. Atanackovic, B. J. Eggleton, and D. J. Moss, Opt. Express **19**(16), 15212 (2011).
[9]A. Spott, Y. Liu, T. Baehr-Jones, R. Ilic, and M. Hochberg, Appl. Phys. Lett. **97**(21), 213501 (2010).
[10]C. Y. Wong, Z. Cheng, X. Chen, K. Xu, C. K. Y. Fung, Y. M. Chen, and H. K. Tsang, IEEE Photon. J. **4**(4), 1095 (2012).
[11]S. J. McNab, N. Moll, and Y. A. Vlasov, Opt. Express **11**(22), 2927 (2003).
[12]D. Vermeulen, S. Selvaraja, P. Verheyen, G. Lepage, W. Bogaerts, P. Absil, D. Van Thourhout, and G. Roelkens, Opt. Express **18**(17), 18278 (2010).
[13]X. Chen, K. Xu, Z. Z. Cheng, C. K. Y. Fung, and H. K. Tsang, Opt. Lett. **37**(17), 3483 (2012).
[14]S. Le Digabel, Acm Trans. Math. Softw. **37**(4), 14 (2011).
[15]T. J. Kippenberg, S. M. Spillane, and K. J. Vahala, Opt. Lett. **27**(19), 1669 (2002).
[16]M. Borselli, T. J. Johnson, and O. Painter, Appl. Phys. Lett. **88**(13), 131114 (2006).
[17]M. Borselli, T. J. Johnson, and O. Painter, Opt. Express **13**(5), 1515 (2005).
[18]G. Z. Mashanovich, M. M. Milosevic, M. Nedeljkovic, N. Owens, B. Q. Xiong, E. J. Teo, and Y. F. Hu, Opt. Express **19**(8), 7112 (2011).
[19]G. Imthurn, "The History of Silicon-on-Sapphire," white paper for Peregrine Semiconductor Corporation, 2007.